Bioorganic & Medicinal Chemistry Letters 21 (2011) 6678–6686

Contents lists available at SciVerse ScienceDirect

Bioorganic & Medicinal Chemistry Letters

journal homepage: www.elsevier.com/locate/bmcl

# Synthesis of polyfunctionalized piperidone oxime ethers and their cytotoxicity on HeLa cells

Paramasivam Parthiban [a,b], Ramjee Pallela [c], Se-Kwon Kim [c], Dong Ho Park [a], Yeon Tae Jeong [b,*]

[a] Department of Biomedicinal Chemistry, Inje University, Gimhae 621 749, Gyeongnam, South Korea
[b] Division of Image Science and Engineering, Pukyong National University, Busan 608 737, South Korea
[c] Marine Bioprocess Research Center, Pukyong National University, Nam-Gu, Busan 608 737, South Korea

ARTICLE INFO

*Article history:*
Received 29 May 2011
Revised 29 July 2011
Accepted 16 September 2011
Available online 21 September 2011

*Keywords:*
Polyfunctionalized piperidin-4-ones
Stereochemistry
Epimerization
HeLa cells
Cytotoxicity
MTT assay

ABSTRACT

A series of twenty 2,6-diarylpiperidin-4-one *O*-methyloximes were synthesized with fluoro/chloro/bromo/methyl/methoxy/ethoxy/isopropyl substituents on various positions of the phenyl at C-2 and C-6 in association with/without methyl substituent on the secondary amino group and methyl/ethyl/isopropyl substituents on the active methylene centers. Regardless of their substitution all compounds predominantly exist in the chair conformation except **3m**, which adopts a twist-boat conformation. All the synthesized compounds were evaluated for their in vitro antiproliferative activity against human cervical carcinoma (HeLa) cell line. The cytotoxicity of the test compounds was determined by measuring the number of live cells after 24 h of treatment by MTT assay method. This preliminary SAR suggests some lead molecules **3c–f**, **3j–k**, **4d–g**, and **4i** with a scope of further structural optimization of the piperidone pharmacophore toward the development of anticancer drug synthesis.



Nitrogen containing heterocycles always signified a subject of great interest due to their ubiquity in nature and massive presence as part of the skeletal backbone of many therapeutic agents.[1] Of these heterocycles, piperidone pharmacophore is very momentous by its broad-spectrum of biological actions.[2] Introduction of various substituents on the piperidone heterocycle and reduction of the carbonyl as oxime functionality improved the biological efficacy.[3] As a part of our ongoing research[4] toward the development of new piperidone based compounds with structure diversity, for this study, 2,6-diphenylperidin-4-one *O*-methyloxime **3a**, 3-alkyl analogs **3b–j**, 3,5-dimethyl analogs **3k–o** and some *N*-methyl analogs **4d–i** were synthesized as depicted in Scheme 1.

All compounds were characterized by their analytical and spectral data, and thus their stereochemistries are established.[5] Compound **3a** has no substitution on the heterocycle other than the phenyl rings at C-2 and C-6, which paved the secondary amino group. The vicinal couplings clearly suggest that **3a** adopts a chair conformation with an equatorial orientation of the phenyl rings on both sides of the secondary amino group. Introduction of a methyl group at C-3 of **3a** along with/without halo/alkyl/alkoxy substituents on the phenyl at C-2 and C-6 (**3b–h**) did not alter the stereochemistry. Likewise, the introduction of methyl group at ring nitrogen of **3d–h** also did not alter the stereochemistry of **4d–h**. Both the methyl groups at N-1 and C-3 preferred the equatorial disposition. Similarly to methyl, the introduction of ethyl **3i** and isopropyl **3j** groups at C-3 of **3a** also did not affect the stereochemistry significantly. They also adopt the analogous stereochemistry as **3b**. However, the decrease in the $^{3}J_{2a,3a}$ of **3j** indicates that there may be a least possible population of boat conformation for **3j** and its *N*-methyl analog **4i**.

On the other hand, the incorporation of methyl group on both sides of the active methylene centers C-3 and C-5 partially/completely modify the stereochemistry of the synthesized compounds **3k–o**. Although the 3,5-dimethyl substituted piperidones **1k–o** exist in the chair conformation with an equatorial orientation of all substituents, the oxime derivatives **3k**, **3l**, **3n** and **3o** underwent epimerization to retain the chair conformation. One of the methyl groups, which is *syn* to the oxime moiety was epimerized to adopt an axial orientation at C-5 to stabilize the chair conformation. In fact, in order to relieve from the severe allylic 1,3-interaction between the methyl at C-5 and N–O, the methyl at C-5 was epimerized. But a prominent change was noticed on compound **3m**, which underwent a conformational transformation instead of the epimerization observed in analogous compounds and thus adopts a twist-boat conformation.

All the synthesized compounds **3a–4i** were evaluated for their in vitro antiproliferative activity against human cervical carcinoma (HeLa) cell line. The cytotoxicity of the test compounds was determined by measuring the number of live cells after 24 h of treatment by MTT assay.[6] The $IC_{50}$ values of all compounds are summarized along with their stereochemical structures in Table 1 for better

* Corresponding author.
*E-mail address:* ytjeong@pknu.ac.kr (Y.T. Jeong).

0960-894X/$ - see front matter © 2011 Elsevier Ltd. All rights reserved.
doi:10.1016/j.bmcl.2011.09.063

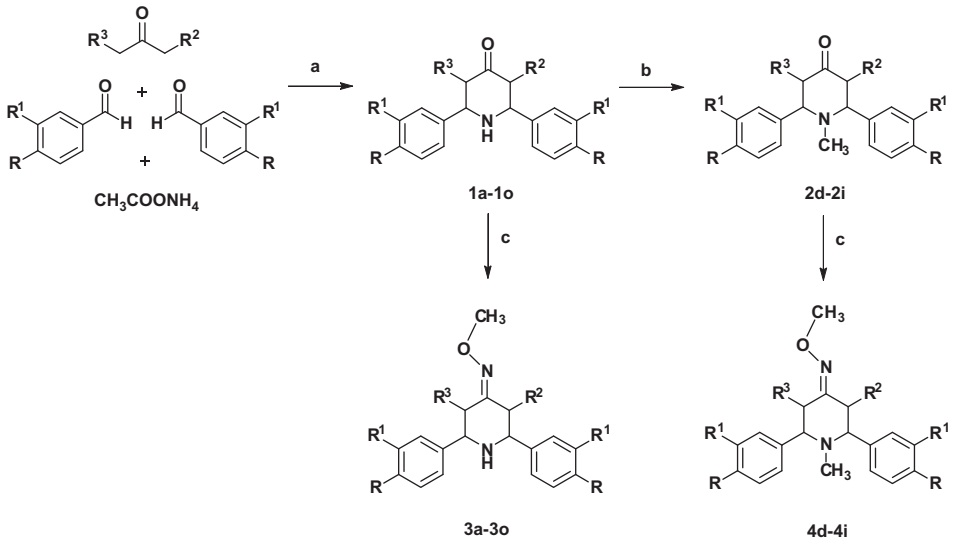


| Entry | R | $R^1$ | $R^2$ | $R^3$ | Entry | R | $R^1$ | $R^2$ | $R^3$ |
|---|---|---|---|---|---|---|---|---|---|
| **a** | H | H | H | H | **i** | H | H | $CH_2CH_3$ | H |
| **b** | H | H | $CH_3$ | H | **j** | H | H | $CH(CH_3)_2$ | H |
| **c** | Br | H | $CH_3$ | H | **k** | H | F | $CH_3$ | $CH_3$ |
| **d** | Cl | H | $CH_3$ | H | **l** | $CH_3$ | H | $CH_3$ | $CH_3$ |
| **e** | F | H | $CH_3$ | H | **m** | $CH(CH_3)_2$ | H | $CH_3$ | $CH_3$ |
| **f** | H | F | $CH_3$ | H | **n** | $OCH_3$ | H | $CH_3$ | $CH_3$ |
| **g** | $CH_3$ | H | $CH_3$ | H | **o** | $OCH_2CH_3$ | H | $CH_3$ | $CH_3$ |
| **h** | $OCH_3$ | H | $CH_3$ | H | | | | | |

**Scheme 1.** Reagents and conditions: (a) Ethanol/warm; (b) methyl iodide/anhydrous $K_2CO_3$/dry acetone/reflux; (c) methoxylamine hydrochloride/sodium acetate trihydrate/ethanol/reflux.

structure–activity comprehension. Besides, the standard drugs Camptothecin and Etoposide were also analyzed under identical conditions and their $IC_{50}$ values are also reproduced in the Table 1.

The HeLa cell line was obtained from American Type Culture Collection (Manassas, VA, USA). Dulbecco's Modified Eagle's Medium (DMEM) was purchased from BioWhittaker®, whereas fetal bovine serum (FBS) and other cell culture materials were purchased from Gibco BRL Life Technologies, USA. Paraformaldehyde and Bisbenzimide Hoechst 33342 stain were procured from Sigma–Aldrich Corp., St. Louis, MO, USA, and MTT [3-(4,5-dimethylthiazol-2-yl)-2,5-diphenyltetrasolium bromide] was purchased from Biosesang Inc., Korea.

Cells were cultured in T-75 tissue culture flasks (Nunc, Denmark) at 37 °C in a 5% $CO_2$ humidified incubator using appropriate media supplemented with DMEM containing 10% heat-inactivated FBS, 100 units/mL Penicillin and 100 μg/mL Streptomycin. Cells were seeded in a 96 well microtiter plate containing 100 μL medium at a final density of $2 \times 10^4$ cells/well at identical conditions. After overnight incubation, the cells were treated with different concentrations of test compounds (6.25–100 μg/mL) or DMSO (carrier solvent) in a final volume of 200 μL. After 24 h, 10 μL of MTT (5 mg/mL) was added to each well and the plate was incubated at 37 °C in the dark for 4 h. Then the media along with MTT was removed and the formazan crystals were solubilized by adding DMSO (100 μL/well). Finally, the reduction of MTT was quantified by reading the absorbance at 570 nm by GENios® microplate reader (Tecan Austria GmbH). Effects of the test compounds on cell viability were calculated using cells treated with DMSO as control. The data were subjected to linear regression analysis and the regression lines were plotted for the best straight-line fit. The $IC_{50}$ (inhibition of cell viability to 50%) concentrations were calculated using the respective regression equation as shown in Table 1.

A careful analysis of Table 1 provides the structure–activity correlations as indicated by their $IC_{50}$ values. Compound **3a** is a simple piperidone molecule and it has no substitution on the phenyl as well as active methylene centers and ring nitrogen, which shows activity at an $IC_{50}$ of 121 μM. The introduction of a methyl group on one of the active methylene centers of the piperidone moiety **3a** affords **3b**, which fairly improves the efficacy as noticed $IC_{50}$ of 113 μM. However, the replacement of methyl by ethyl **3i** shows an incredible improvement in its efficacy ($IC_{50}$ 57 μM). Similarly, the replacement of methyl by isopropyl **3j** exhibits activity at an $IC_{50}$ of 49 μM. Further the incorporation of a methyl group at the ring nitrogen of **3i** improved the $IC_{50}$ of **4i** from 57 to 41 μM.

A remarkable improvement is observed by the introduction of a bromo substituent on *para*-position of the phenyl at C-2 and C-6 (**3c**), which discloses an excellent inhibition of the growth of the HeLa cells at an $IC_{50}$ of 25.02 μM in 24 h. This $IC_{50}$ is nearly three-fold higher than the standard drug Camptothecin (8.93 μM); however, it is very closer and even comparable to the Etoposide standard (23.33 μM). The replacement of *para*-bromo

**Table 1**
[a]Cytotoxic effect of compounds **3a**–**4i** on HeLa cells

| Compound | Structure | Yield | [b]Linear regression equation [log]: $Y = A + Bx$ | $R$ value | [c]$IC_{50}$ in μM |
|---|---|---|---|---|---|
| **3a** | 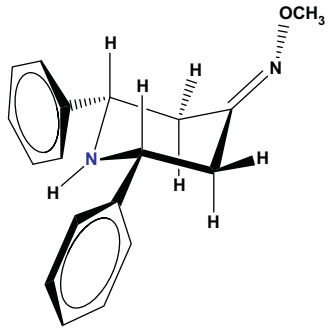 | 96 | $Y = -59.47669 + (70.42453)x$ | 0.97 | 120.68 ± 15.03 |
| **3b** | 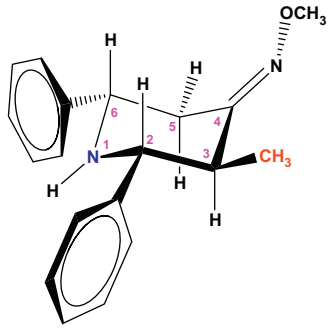 | 95 | $Y = -51.73964 + (66.89936)x$ | 0.97 | 112.72 ± 2.27 |
| **3c** | 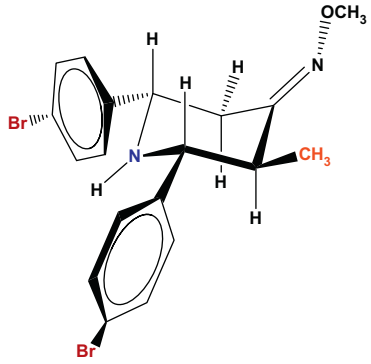 | 93 | $Y = 4.00027 + (43.70457)x$ | 0.99 | 25.02 ± 2.07 |
| **3d** | 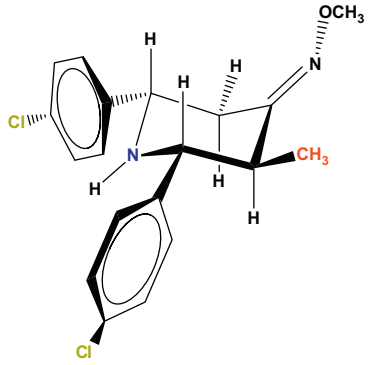 | 93 | $Y = -2.07215 + (41.57979)x$ | 0.99 | 48.97 ± 6.6 |

**Table 1** (*continued*)

| Compound | Structure | Yield | [b]Linear regression equation [log]: $Y = A + Bx$ | $R$ value | [c]$IC_{50}$ in μM |
|---|---|---|---|---|---|
| **3e** | 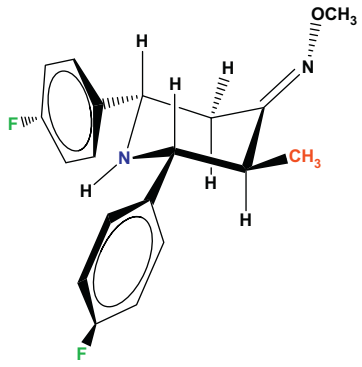 | 94 | $Y = -20.54996 + (58.6915)x$ | 0.99 | 49.18 ± 2.14 |
| **3f** | 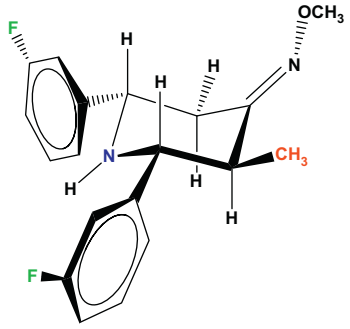 | 89 | $Y = -9.32307 + (51.13401)x$ | 0.99 | 38.42 ± 7.55 |
| **3g** | 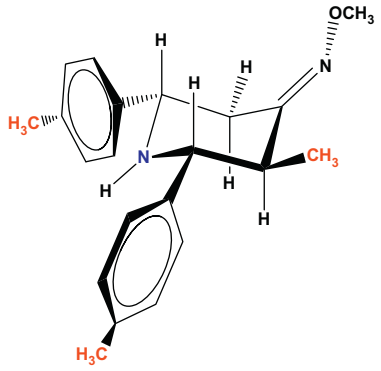 | 93 | $Y = -34.93378 + (59.77543)x$ | 0.98 | 81.64 ± 4.05 |
| **3h** | 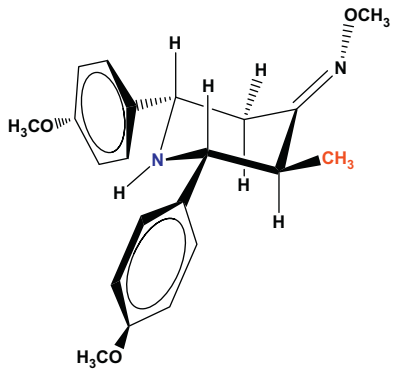 | 95 | $Y = -57.94737 + (62.12321)x$ | 0.97 | 154.34 ± 8.06 |

(*continued on next page*)

**Table 1** (*continued*)

| Compound | Structure | Yield | [b]Linear regression equation [log]: $Y = A + Bx$ | $R$ value | [c]$IC_{50}$ in μM |
|---|---|---|---|---|---|
| **3i** | 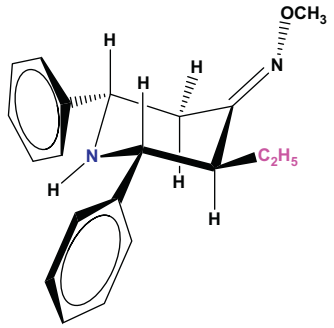 | 95 | $Y = -45.72953 + (73.21416)x$ | 0.97 | 57.27 ± 3.85 |
| **3j** | 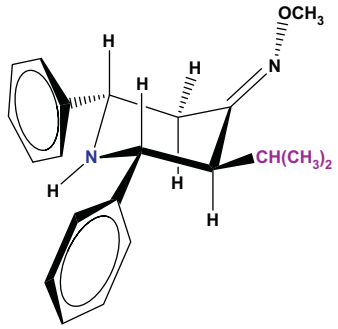 | 93 | $Y = -17.80104 + (56.36107)x$ | 0.96 | 49.54 ± 1.62 |
| **3k** | 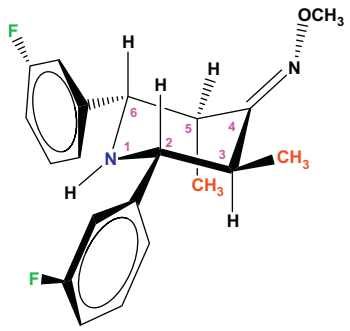 | 85 | $Y = 0.09372 + (44.63047)x$ | 0.99 | 37.86 ± 5.05 |
| **3l** | 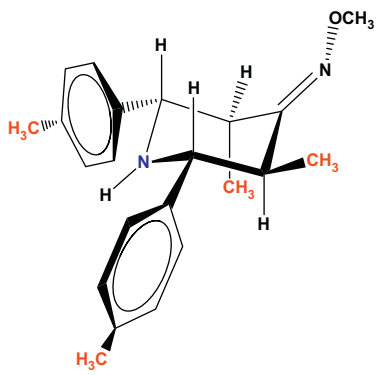 | 78 | $Y = -30.78913 + (63.75446)x$ | 0.98 | 54.88 ± 3.46 |

**Table 1** (*continued*)

| Compound | Structure | Yield | [b]Linear regression equation [log]: $Y = A + Bx$ | $R$ value | [c]$IC_{50}$ in μM |
|---|---|---|---|---|---|
| **3m** | 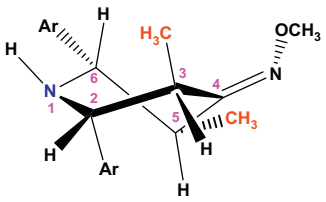 Ar = *para*-$CH(CH_3)_2Ph$ | 55 | $Y = -13.53982 + (48.80922)x$ | 0.98 | 50.96 ± 1.61 |
| **3n** | 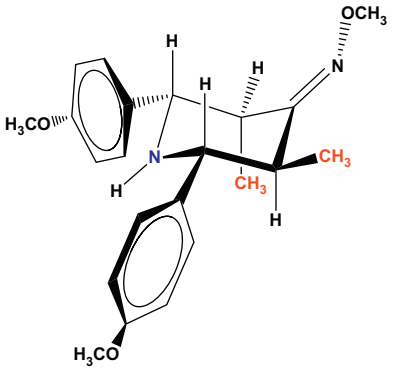 | 76 | $Y = -35.01759 + (55.23339)x$ | 0.96 | 93.91 ± 3.38 |
| **3o** | 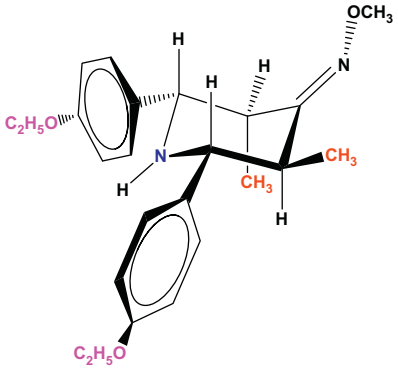 | 71 | $Y = -35.39224 + (53.82258)x$ | 0.97 | 98.02 ± 9.74 |
| **4d** | 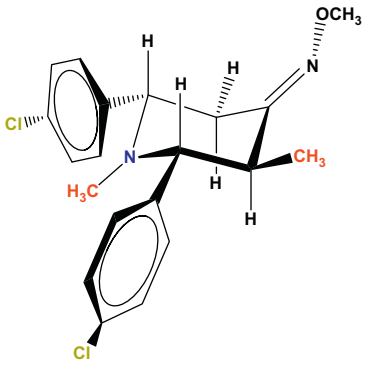 | 90 | $Y = -21.30888 + (62.78321)x$ | 0.97 | 36.27 ± 1.94 |

(*continued on next page*)

**Table 1** (*continued*)

| Compound | Structure | Yield | [b]Linear regression equation [log]: $Y = A + Bx$ | $R$ value | [c]$IC_{50}$ in μM |
|---|---|---|---|---|---|
| **4e** | 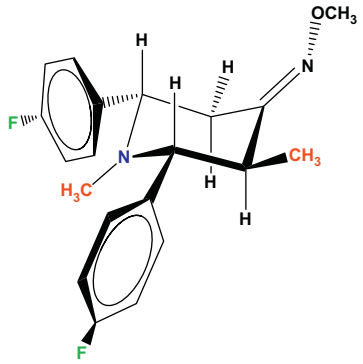 | 91 | $Y = -25.19937 + (65.48558)x$ | 0.97 | 40.73 ± 2.63 |
| **4g** | 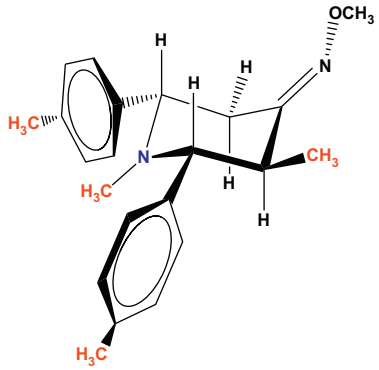 | 91 | $Y = -19.85852 + (58.03169)x$ | 0.99 | 47.68 ± 2.94 |
| **4h** | 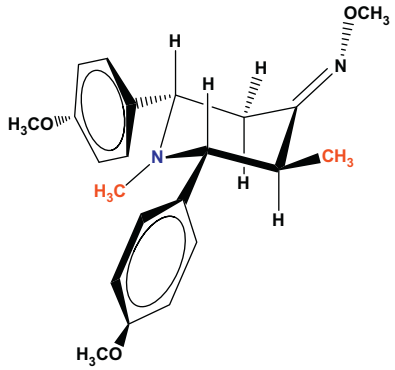 | 92 | $Y = -19.31948 + (47.05231)x$ | 0.96 | 80.62 ± 5.33 |
| **4i** | 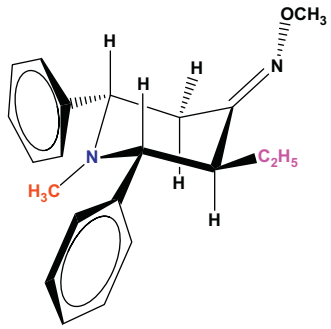 | 93 | $Y = -0.933 + (45.94471)x$ | 0.99 | 41.69 ± 7.05 |
| Camptothecin | | | $Y = 29.02966 + (42.56504)x$ | 0.99 | 8.93 ± 0.54 |
| Etoposide | | | $Y = 2.27708 + (41.80905)x$ | 0.98 | 23.33 ± 0.92 |

[a] Exponentially growing cells were treated with different concentrations of test compounds for 24 h and cell growth inhibition was analyzed through MTT assay.

[b] Mean percent decrease in cell number of five independent experiments was used to calculate the linear regression equation. Linear regression: $Y = A + Bx$ ($A$ = $Y$-intercept; $B$ = slope of the line; $x$ = x-scale).

[c] $IC_{50}$ is defined as the concentration, which results in a 50% decrease in cell number as compared with that of the control cultures in the absence of an inhibitor. The values represent the mean ± SD of five individual observations.

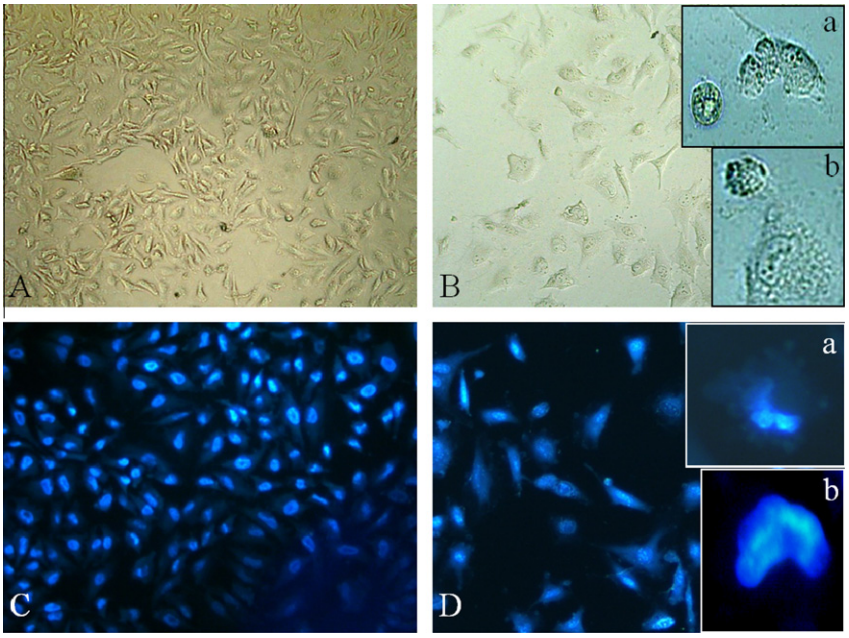


**Figure 1.** Light and fluorescent micrographs of normal and treated HeLa cells. Phase contrast microscope images of (A) normal cells (B) the cells treated with $IC_{50}$ concentration (25 μM) of the most active lead compound **3c**. Early signs of apoptosis was characterized by the blebbing of cell membrane (*inset* a) followed by cell membrane destruction (*inset* b). Fluorescence microscope images of (C) normal cells (D) the cells treated with 25 μM of **3c**, stained with Hoechst 33342. Extremely condensed chromatin (Pyknotic nuclei) is marginated into a horseshoe-shaped structure (*inset* a & b). The cells were detected by fluorescence light microscopy at 360 nm/470 nm excitation/emission.

by chloro (**3d**) or fluoro (**3e**) decrease its efficiency nearly to half but the N-methylation of **3d** and **3e** register an enhanced efficacy ($IC_{50}$ of **4d** and **4e** are 36 and 41 μM, respectively) than their non-methylated counterparts. Analogously, a two-fold improvement is observed for **4g**–**h** ($IC_{50}$ 48 and 81 μM) by the N-methylation on **3g**–**h**.

The positional isomer of **3e**, that is, compound **3f** shows an improvement in its inhibition from the $IC_{50}$ of 49 to 38 μM and a further improvement noticed by the incorporation of another methyl group on another active methylene center. Though it is less for **3k**, a remarkable progress observed for compounds **3l** and **3n** (55 and 94 μM, respectively) than **3g** (82 μM) and **3h** (154 μM) by the insertion of methyl on both the active methylene centers C-3 and C-5; in fact, nearly a two-fold improvement in their efficiency. The replacement of *para*-methyl by *para*-isopropyl in **3l** (55 μM) provides only a marginal improvement ($IC_{50}$ of **3m** is 51 μM).

The altered morphology of exposed cells ($1 \times 10^5$/well) at different concentrations was studied after 24 h using phase contrast microscope (DMI6000B, Leica Microsystems, Wetzlar, Germany). Subsequently, the cells were Hoechst stained to observe the nuclear/chromosomal condensation occurred by the treatment of the test compound. For staining the cells, 96 well microtiter plates were used to culture the cells ($1 \times 10^4$ cells/well) in three replicates to treat with the ideal lead compound **3c**. Then the cells were incubated at 37 °C for overnight and the media was removed to wash the cells twice with phosphate buffered saline (PBS) and fixed with 4% paraformaldehyde in PBS for one day at −4 °C. Further, the cells were stained with 1 μg/mL of the fluorescent DNA-binding dye, Bisbenzimide Hoechst 33342 stain and incubated for 20 min at room temperature to reveal nuclear condensation/aggregation due to the effect of the test compound. The Hoechst-stained cells were visualized and photographed under fluorescence microscope (CTR 6000; Leica, Wetzlar, Germany) and reproduced in Figure 1.

The cytomorphological abnormalities occurred by the effect of the lead compound **3c** were observed under a phase contrast microscope. The control showed normal healthy and intact nuclei without any cytomorphological abnormalities (Fig. 1A). The cells treated with $IC_{50}$ concentration (25 μM) of **3c** for 24 h showed evident morphological changes with blebbing of cellular membrane, chromatin condensation and fragmentation followed by the formation of apoptotic bodies (Fig. 1B, inset a). Most of the treated cells exhibited the symptoms of apoptosis but the damage was severe in some cells, with the cell membrane rupture and the subsequent release of cytoplasm as observed in Figure 1B (inset b). The above results of light microscopy were consistent with that of fluorescence microscopy using Hoechst 33342 stain for control and treated cells (Figs. 1C and D, respectively). Bright condensed chromatin (pyknosis) was observed in the **3c** treated cells, which represents the early signs of apoptosis. This leads to a deformed nucleus/cytoplasm consistency and the margination of chromatin into a horseshoe shaped structure (Fig. 1D, inset 'a' and 'b'). Consequent to this process, fragmentation of the nucleus (karyorrhexis) was also observed in the treated cells.

The structure–activity correlations indicate the improvement in $IC_{50}$ by the substitution of methyl on both the active methylene centers and secondary amino group besides the halo substitution on the phenyl groups. As a result, the preliminary investigation suggests some lead molecules with good cytotoxicity of <50 μM of $IC_{50}$ after 24 h against the HeLa cells. Particularly, **3c** exhibits an $IC_{50}$ of 25.02 μM and is comparable to the standard drug Etoposide (23.33 μM); thus deserves further structural optimization of this pharmacophore to attain betterment in the anticancer drug synthesis.

## References and notes

1. Pelletier, S. W. *Chemistry of Alkaloids*; Van Nostrand: New York, 1970; (b) Jeyaraman, R.; Avila, S. *Chem. Rev.* **1981**, *81*, 149; (c) Schneider, M. J. In *Alkaloids: Chemical and Biological Perspectives*; Pelletier, S. W., Ed.; Wiley: New York, 1996.
2. (a) Baliah, V.; Jeyaraman, R.; Chandrasekaran, L. *Chem. Rev.* **1983**, *83*, 379; (b) Reddy, P. A.; Woodward, K. E.; Mcllheran, S. M.; Hsiang, B. C. H.; Latifi, T. N.; Hill, M. W. *J. Med. Chem.* **1997**, *40*, 44; (c) Parthiban, P.; Balasubramanian, S.; Aridoss, G.; Kabilan, S. *Med. Chem. Res.* **2005**, *14*, 523; (d) Kumar, R. R.; Perumal, S.; Senthilkumar, P.; Yogeeswari, P.; Sriram, D. *Eur. J. Med. Chem.* **2009**, *44*, 3821; (e) Girgis, A. S. *Eur. J. Med. Chem.* **2009**, *44*, 1257; (f) Youssef, D.; Potter, E.; Jha, M.;

Clercq, E. D.; James, J. B.; Stables, P.; Jha, A. *Bioorg. Med. Chem. Lett.* **2009**, *19*, 6364; (g) Karthikeyan, N. S.; Sathiyanarayanan, K. I.; Aravindan, P. G.; Giridharan, P. *Med. Chem. Res.* **2011**, *20*, 81.

3. (a) Lijinsky, W.; Taylor, H. W. *Int. J. Cancer* **1975**, *16*, 318; (b) Prostakov, N. S.; Gaivoronskaya, L. A. *Chem. Rev.* **1978**, *47*, 447; (c) Balasubramanian, S.; Aridoss, G.; Parthiban, P.; Ramalingan, C.; Kabilan, S. *Biol. Pharm. Bull.* **2006**, *29*, 125; (d) Parthiban, P.; Aridoss, G.; Rathika, P.; Ramkumar, V.; Kabilan, S. *Bioorg. Med. Chem. Lett.* **2009**, *19*, 2981.
4. (a) Parthiban, P.; Balasubramanian, S.; Aridoss, G.; Kabilan, S. *Spectrochim. Acta, Part A* **2008**, *70*, 11; (b) Parthiban, P.; Rani, M.; Kabilan, S. *Monatsh. Chem.* **2009**, *140*, 287; (c) Dindulkar, S. D.; Parthiban, P.; Purnik, V. G.; Jeong, Y. T. *J. Mol. Struct.* **2011**, *990*, 44.
5. *Analytical and spectral data of some representative compounds:* **3a**: *r*-2,*c*-6-Diphenylpiperidin-4-one *O*-methyloxime. Off-white semi-solid, yield 96%; $^1$H NMR: $\delta$ = 3.94 (dd, $J_{2a,3a}$ = 11.72 Hz; $J_{2a,3e}$ = 2.56 Hz, 1H, H-2a), 3.86 (dd, H-6a, overlapped with the methyl protons of oxime ether moiety), 3.44 (td, $J_{5e,6a}$ = 13.92 Hz, 1H, H-5e), 2.58 (td, $J_{3e,2a}$ = 13.56 Hz, 1H, H-3e), 2.35 (t, $J_{3a,3e}$ = 12.84 Hz, $J_{3a,2a}$ = 12.08 Hz 1H, H-3a), 1.99 (t, $J_{5a,5e}$ = 12.84 Hz, $J_{5a,6a}$ = 12.44 Hz 1H, H-5a), 1.92 (br s, 1H, merged with H-5a), 3.86 (s, $CH_3$ of oxime ether), 7.48 (dd, 4H, H-2″ and H-6″, $J$ = 6.76, 4.80 Hz), 7.35 (t, 4H, H-2‴ and H-6‴, $J$ = 7.32, 7.68 Hz), 7.29 (d, 2H, H-2⁗ and H-6⁗, $J$ = 7.32 Hz) ppm; $^{13}$C NMR: $\delta$ = 62.16 (C-2), 60.81 (C-6), 40.53 (C-3), 34.02 (C-5), 157.25 (C=N), 61.37 ($CH_3$ of oxime ether), 143.65 (C-2′), 143.58 (C-6′), 128.72, 128.69, 127.80, 126.86, 126.77 (other aryl carbons) ppm; IR: 1637 (C=N stretching) cm$^{-1}$; HRMS: *m*/*z*:281.15 [*M*+H]$^+$; Anal. Cacld for $C_{18}H_{20}N_2O$: C, 77.11; H, 7.19; N, 9.99. Found: C, 77.10; H, 7.20; N, 10.00; **3b**: *t*-3-Methyl-*r*-2,*c*-6-diphenylpiperidin-4-one *O*-methyloxime. Faint yellow semi-solid, yield 95%; $^1$H NMR: $\delta$ = 3.53 (m, d of H-2a and dd of H-5e are overlapped), 3.88 (dd of H-6a overlapped with the methyl protons of oxime ether), 2.53 (sextet, 1H, H-3a), 2.01 (t, H-5a), 1.87 (s, 1H, NH), 0.88 (d, $J$ = 6.24 Hz, 3H, $CH_3$ at C-3), 3.87 (s, $CH_3$ of oxime ether), 7.45 (t, 4H, H-2″ and H-6″), 7.37–7.26 (m, 6H, H-2‴, H-6‴, H-2⁗ and H-6⁗) ppm; $^{13}$C NMR: $\delta$ = 69.36 (C-2), 60.89 (C-6), 42.92 (C-3), 34.16 (C-5), 159.39 (C=N), 61.67 ($CH_3$ of oxime ether), 11.96 ($CH_3$ at C-3), 142.24 (C-2′), 143.31 (C-6′), 128.55, 128.48, 128.12, 128.05, 127.70, 126.82 (other aryl carbons) ppm; IR: 1642 (C=N stretching) cm$^{-1}$; HRMS: *m*/*z*: 295.17 [*M*+H]$^+$; Anal. Cacld for $C_{19}H_{22}N_2O$: C, 77.52; H, 7.53; N, 9.52. Found: C, 77.50; H, 7.52; N, 9.50; **3c**: *t*-3-Methyl-*r*-2,*c*-6-*bis*(4-bromophenyl)piperidin-4-one *O*-methyloxime. Brown semi-solid, yield 93%; $^1$H NMR: $\delta$ = 3.82 (dd, $J_{5a,6a}$ = 11.72 Hz; $J_{6a,5e}$ = 2.92 Hz, 1H, H-6a), 3.50–3.46 (m, 2H, d of H-6a and dd of H-5e are overlapped), 2.40 (sextet, 1H, H-3a), 1.90 (dd, $J_{5e,5a}$ = 13.56 Hz; $J_{5a,6a}$ = 11.72 Hz, 1H, H-5a), 1.77 (br s, 1H, NH), 0.86 (d, $J$ = 6.60 Hz, 3H, $CH_3$ at C-3), 3.86 (s, 3H, $CH_3$ of oxime ether), 7.45 (dd, 4H, $J$ = 10.24, 8.44 Hz), 7.32 (dd, 4H, $J$ = 8.76, 2.56 Hz) ppm; $^{13}$C NMR: $\delta$ = 68.58 (C-2), 60.15 (C-6), 43.09 (C-3), 34.36 (C-5), 158.51 (C=N), 61.41 ($CH_3$ of oxime ether), 11.82 ($CH_3$ at C-3), 141.56 (C-2'), 142.67 (C-6'), 121.34 (C-2‴), 121.63 (C-6⁗), 131.65, 131.60, 129.66, 128.44 (other aryl carbons) ppm; IR: 1637 (C=N stretching) cm$^{-1}$; HRMS: *m*/*z*: 451.00 [*M*+H]$^+$; Anal. Cacld for $C_{19}H_{20}N_2OBr_2$: C, 50.47; H, 4.46; N, 6.20. Found C, 50.50; H, 4.45; N, 6.21; **3d**: *t*-3-Methyl-*r*-2,*c*-6-*bis*(4-chlorophenyl)piperidin-4-one *O*-methyloxime. Pale yellow semi-solid, yield 93%; $^1$H NMR: $\delta$ = 3.83 (dd, $J_{5a,6a}$ = 11.72 Hz; $J_{5e,6a}$ = 2.92 Hz, 1H, H-6a), 3.50–3.46 (2H, d of H-2a and dd of H-5e are overlapped), 2.40 (m, 1H, H-3a), 1.91 (dd, $J_{5e,5a}$ = 13.56 Hz; $J_{5a,6a}$ = 11.72 Hz,1H, H-5a), 1.82 (br s, 1H, NH), 0.86 (d, $J$ = 6.60 Hz, 3H, $CH_3$ at C-3), 3.86 (s, 3H, $CH_3$ of oxime ether), 7.38 (dd, $J$ = 8.10, 1.80 Hz, 4H, H-2″ and H-6″), 7.31 (d, $J$ = 9.88 Hz, 2H, H-2‴), 7.29 (d, $J$ = 8.44 Hz, 2H H-6⁗) ppm; $^{13}$C NMR: $\delta$ = 68.50 (C-2), 60.08 (C-6), 43.14 (C-3), 34.42 (C-5), 158.51 (C=N), 11.79 ($CH_3$ at C-3), 61.34 ($CH_3$ of oxime ether), 141.09 (C-2'), 142.20 (C-6'), 133.15 (C-2‴), 133.42 (C-6⁗), 129.26, 128.66, 128.59, 128.05 (other aryl carbons) ppm; IR: 1637 (C=N stretching) cm$^{-1}$; HRMS: *m*/*z*: 363.10 [*M*+H]$^+$; Anal. Cacld for $C_{19}H_{20}Cl_2N_2O$: C, 62.82; H, 5.55; N, 7.71. Found C, 62.79; H, 5.52; N, 7.70; **3m**: 3,5-Dimethyl-2,6-bis(4-isopropylphenyl)piperidin-4-one *O*-methyloxime. Colorless semi-solid, yield 55%; $^1$H NMR: $\delta$ = 3.75 (d, $J_{2,3}$ = 5.84 Hz, 1H, H-2), 3.64 (d, $J_{5,6}$ = 9.16 Hz, 1H, H-6), 3.20 (quintet, 1H, H-5), 2.79 (quintet, 1H, H-3), 1.28 (d, $J$ = 7.5 Hz, 3H, $CH_3$ at C-3), 1.15 (d, $J$ = 6.96 Hz, 3H, $CH_3$ at C-5), 3.83 (s, 3H, $CH_3$ of oxime ether), 2.95–2.83 (m, 2H, CH of $^i$Pr), 1.23 (d, $J$ = 6.96 Hz, 12H, $CH_3$ of $^i$Pr), 7.20 (dd, 4H, H-2‴ and H-6‴), 7.36 (dd, 4H, H-2'' and H-6'') ppm; $^{13}$C NMR: $\delta$ = 67.88 (C-2), 66.56 (C-6), 42.59 (C-3), 40.00 (C-5), 164.39 (C=N), 21.16 ($CH_3$ at C-3), 15.90 ($CH_3$ at C-5), 61.30 ($CH_3$ of oxime ether), 33.89 (CH of $^i$Pr), 24.12 ($CH_3$ of $^i$Pr), 141.13 (C-2'), 142.41 (C-6'), 148.34, 148.29 (C-2"" and C-6""), 127.93, 127.54, 127.24, 126.92 (other aryl carbons) ppm; IR: 1645 (C=N stretching) cm$^{-1}$; HRMS: *m*/*z*: 392.28 [*M*]$^+$. **3o**: *t*-3,*c*-5-Dimethyl-*r*-2,*c*-6-*bis*(4-ethoxyphenyl)piperidin-4-one *O*-methyloxime. Colorless semi-solid, yield 71%; $^1$H NMR: $\delta$ = 3.42 (d, 1H, H-2a $J_{2a,3a}$ = 10.24 Hz); 4.02 (m, 5H, d of H-6a overlapped with the ethoxy methylene protons); 3.59 (sextet, 1H, H-5e); 2.58 (sextet, 1H, H-3a); 0.92 [d, $J$ = 6.96 Hz, 3H, $CH_3$ at C-5 (ax)], 0.84 [d, $J$ = 6.60 Hz, 3H, $CH_3$ at C-3 (eq)]; 3.88 (s, 3H, $CH_3$ protons of oxime ether); 4.02 (m, –O–$CH_2$–$CH_3$ on the phenyl), 1.41 (m, –O–$CH_2$–$CH_3$ on the phenyl); 7.37 (d, 2H, $J$ = 8.44 Hz), 7.32 (d, 2H, $J$ = 8.80 Hz) (phenyl protons of H-2'' and H-6''); 6.88 (d, 2H, $J$ = 8.40 Hz), 6.86 (d, 2H, $J$ = 8.80 Hz) (phenyl protons of H-2''' and H-6''') ppm; $^{13}$C NMR: $\delta$ = 68.97 (C-2), 62.39 (C-6), 38.87 (C-3), 34.65 (C-5), 164.30 (C=N), 11.90 [$CH_3$ at C-3 (eq)], 11.29 [$CH_3$ at C-5 (ax)], 61.25 ($CH_3$ of oxime ether), 63.39 (-O-$CH_2$-$CH_3$ on the phenyl), 14.88 (–O-$CH_2$-$CH_3$ on the phenyl), 133.94 (C-2'), 135.26 (C-6'), 157.95 (C-2""), 158.51 (C-6""), 128.87, 127.88, 114.38 (other aryl carbons) ppm; IR: 1640 (C=N stretching) cm$^{-1}$; MS (ES): *m*/*z*: 396.24 [*M*]$^+$; Anal. Cacld for $C_{24}H_{32}N_2O_3$: C, 72.70; H, 8.13; N, 7.06. Found C, 72.72; H, 8.16; N, 7.07; **4d**: *t*-1,3-Dimethyl-*r*-2,*c*-6-*bis*(4-chlorophenyl)piperidin-4-one *O*-methyloxime. Viscous liquid, yield 90%; $^1$H NMR: $\delta$ = 2.85 (d, $J_{2a,3a}$ = 10.64 Hz, 1H, H-2a), 3.17 (dd, $J_{5a,6a}$ = 12.08 Hz; $J_{5e,6a}$ = 3.32 Hz, 1H, H-6a), 3.39 (dd, $J_{5e,5a}$ = 13.92 Hz; $J_{5e,6a}$ = 3.32 Hz,1H, H-5e), 2.50 (m, 1H, H-3a), 2.02 (dd, $J_{5e,5a}$ = 13.92 Hz; $J_{5a,6a}$ = 12.08 Hz, 1H, H-5a), 1.68 (s, 1H, N–$CH_3$), 0.79 (d, $J$ = 6.60 Hz, 3H, $CH_3$ at C-3), 3.84 (s, 3H, $CH_3$ of oxime ether), 7.38–7.29 (m, 8H, aryl protons), ppm; $^{13}$C NMR: $\delta$ = 76.96 (C-2), 68.64 (C-6), 43.10 (C-3), 34.95 (C-5), 157.76 (C=N), 12.63 ($CH_3$ at C-3), 41.58 (N–$CH_3$), 61.37 ($CH_3$ of oxime ether), 141.43 (C-2'), 142.77 (C-6'), 132.89 (C-2""), 133.06 (C-6""), 129.48, 128.87, 128.72, 128.51 (other aryl carbons) ppm; IR: 1636 (C=N stretching) cm$^{-1}$; HRMS: *m*/*z*: 376.10 [*M*]$^+$; Anal. Cacld for $C_{20}H_{22}Cl_2N_2O$: C, 63.67; H, 5.88; N, 7.42. Found C, 63.68; H, 5.90; N, 7.40.
6. Mosmann, T. *J. Immunol. Methods* **1983**, *65*, 55.